Journal of Mechanical Engineering Research and Developments
ISSN: 1024-1752
CODEN: JERDFO
Vol. 44, No. 1, pp. 304-316
Published Year 2021

Design and development of the silkscreen printer with an innovative automatic mechanism of feeding and transporting workpieces

Hoang Minh Dang[†], Thanh Kiet Vo[†], Hung Linh Ao[†], Van Binh Phung[‡], Nguyen Viet Duc[‡†*]

[†] Industrial University of Ho Chi Minh City, Ho Chi Minh City, Vietnam
[‡] Le Quy Don Technical University, Hanoi, Vietnam
[‡†] Thuyloi University, 175 Tay Son, Dong Da, Hanoi, Vietnam

*Corresponding author email: ducnv@tlu.edu.vn

ABSTRACT: Demand for printing brands on popular items including pens, cups, bottles, etc. has been increased significantly in the recent years. Therefore, it is necessary to have the machinery to cater to this need. This paper presents the research on design and development of an innovative silkscreen printer with automatic mechanism of feeding and transporting workpieces based on the principle of four-bar parallelogram linkage mechanism. The printer is capable of printing cylindrical items of various diameter and length, performing high productivity with low cost. Dynamic analysis of the feeding and transporting mechanism was carried out to define the motor torque, as well as evaluate the impact and vibration. Mechanical design, control system and overall fabrication and assembly process for the printer were also studied deliberately. After the prototype assembly, the printing experiment showed that the newly silkscreen printer worked well and efficiently. If the real printer involves into a mass production, it would promise to bring great benefits in terms of economy, productivity and labor safety for small and medium-sized printing workshops.

KEYWORDS**:** Silkscreen printer, Four-bar parallelogram linkage mechanism, Dynamic analysis, Mechanical design, Control system.

INTRODUCTION

In the recent years, the competition in the market of consumer goods has increased dramatically, hence the demand for advertising brand names, increasing the aesthetics of products has also intensified. While, screen printing of fine art motifs, product brands on popular items such as pens, cups, bottles, etc. is becoming increasingly urgent. Therefore, more and more automatic silkscreen printers have been studied and manufactured. Up to the present moment, there are few patents regarding this kind of machine, i.e. Milo et al. have introduced a highly industrialized printer with the ability to print with the automation of the combination of printing and drying by the ultraviolet light to ensures that the heat from the drying stage does not dry the ink on the printing frame [1]. While, Mitsunori from Mitsubishi Electric Corporation created the "solar screen printer" [2], in which printing consists of a surface and a vacuum tube, and the surfaces are formed with multiple suction holes and the printed object is placed on the surface, then objects are printed with vacuum (suction holes use vacuum pipes). On the other side, Kacharen et al. [3] and Selase et al. [4] have invented the pneumatic multicolour screen printing machine and the portable T-shirt printing machine respectively. Both of them used compressed air to motivate the movement, the machine is capable of printing multicolors. Yet, when the print frame translates under the impact of friction, the print object will rotate around the axis.

Although there are numerous advantages of currently-existing silkscreen printers, there are still a series of problems that have to be improved. For instance in Vietnam, in order to have a compact machine, currently a vast amount of small and medium-sized businesses use homemade manual silkscreen printers, in which most of the stages handled manually by workers. This machine has low printing productivity, unstable position, and easy pattern error when printing. Thus, it is only appropriate for small-scale deal. To solve this problem, it is possible to implement the industrial printing machine, which yields high printing productivity, time economy, automation. However, this

machine requires high accuracy of processing and assembly, high cost of purchase, huge amount of specified items to print. Besides, it needs to have a big place, because the machine is bulku and it involves a lage working space that is not suitable for small and medium-sized businesses. Based on the evaluation of printing technology and existing silkscreen printers, as well as by mean of Procedure for Automation of Mathematical Modeling and Solution of mechanical system or PAMMS [5], the authors have proposed an innovative silkscreen printer with automatic mechanism of feeding and transporting workpieces. In this printer, the workpiece is situated in slant troughs with slots to navigate the rotating circular print items, it then rolls out of the printing position to exit. The aim and objective in this paper mainly are to present the design, simulation and prototype development of this newly-machine.

COMPUTATION AND SIMULATION OF AUTOMATIC MECHANISM OF FEEDING AND TRANSPORTING WORKPIECE

Principle of mechanism

The mechanism of transporting workpiece is demonstrated in Figure 1. The workpiece (2) rolls on the slant gutter to get into Position 1, then the parallelogram linkage (3) rotates evenly to lift the workpiece to Position 2 in circular orbits, at the same time the next workpiece from the chute will be rolled down into Position 1. Parallelogram linkage (3) moves the next cycle and lift the workpiece from Position 1 to Position 2, Position 3 consecutively, and then the screen printing frame (1) will descend to perform the printing. This process is repeated over and over and forms a closed-loop procedure.

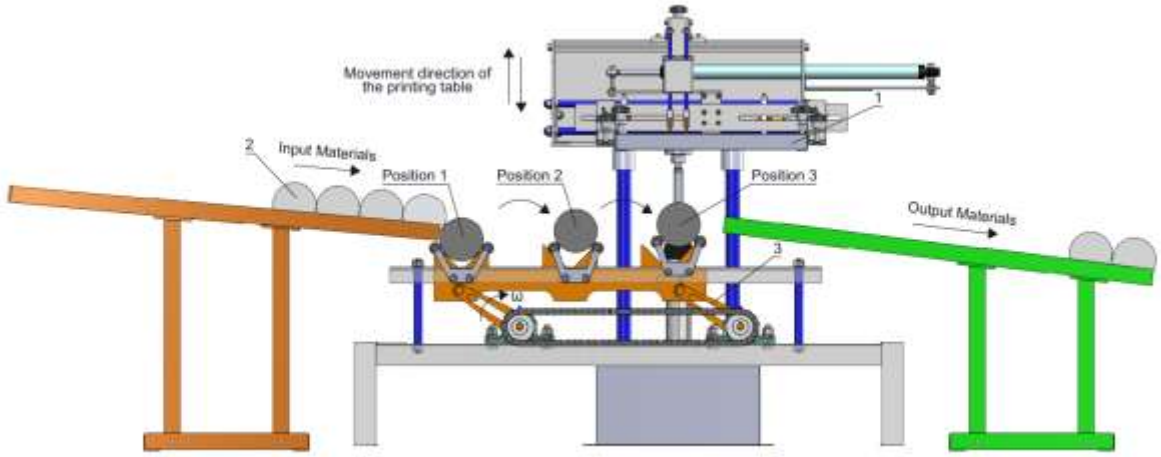

1- Silk screen printing frame; 2- Workpiece; 3 - Parallelogram linkage for workpiece transportation

Figure 1. Principle diagram of the innovative silkscreen printer

Reasons for the selection of a workpiece transporting mechanism with three setting positions are following:

- Case 1: If there are only two setting positions, and the distance one to another is less than 314mm (maximum length of silkscreen printing frame (1) corresponding to the maximum workpiece diameter of 100mm), the frame will intervence with the feeding gutter during descendance, which directly affects printing quality;
- Case 2: If there are only two setting positions, and the distance one to another is greater than 314mm, the rotational trajectory of the parallelogram linkage (3) will be large, leading to high probability of workpiece free fall, which causes damage and lower printing productivity.

Dynamic analysis of transporting workpiece mechanism

The transporting workpiece mechanism plays a crucial role in the silkscreen printer performance. Dynamic analysis and simulation of the mechanism allow for controlling the printer in an easy and reasonable manner. The transporting workpiece mechanism operates by mean of the parallelogram linkage, as shown in Figure 2. Based on dynamic equation of three links *AB*, *BD*, and *DC*, there are:

$$\begin{aligned} &X_A + X_B = A; Y_A + Y_B = B; C \cdot X_A + D \cdot Y_A + E \cdot X_B + F \cdot Y_B = G; X_D - X_B = H; Y_D - Y_B = I; \\ &J \cdot X_B + K \cdot Y_B + L \cdot X_D + N \cdot Y_D = 0; X_C - X_D = P; Y_C - Y_D = Q; R \cdot X_C + S \cdot Y_C + T \cdot X_D + U \cdot Y_D = V. \end{aligned} \quad (1)$$

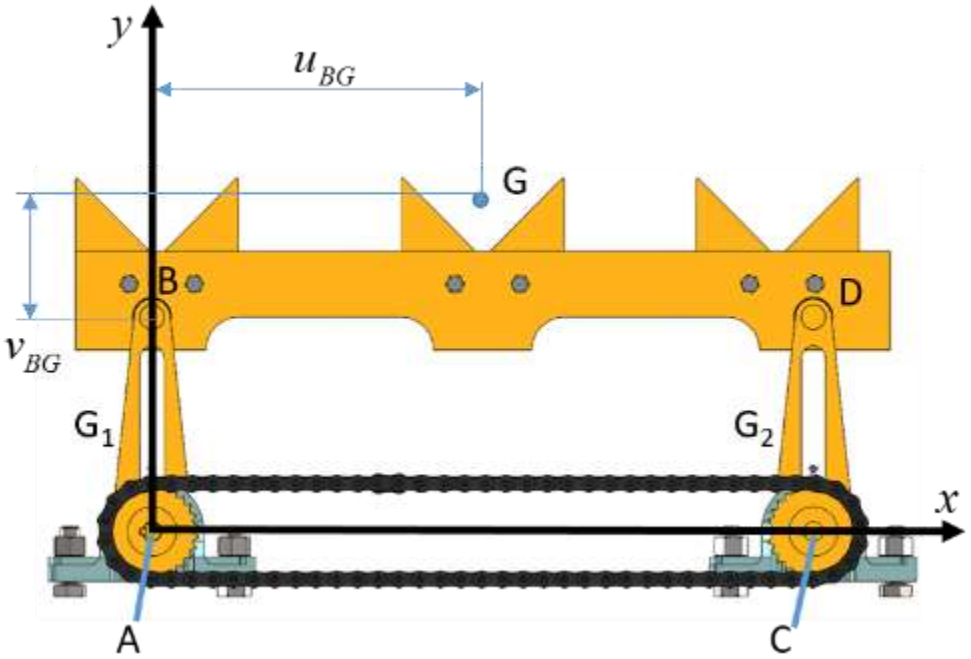

Figure 2. Parallelogram linkage. G_1, G_2, and G are gravity centers of lifting links AB, DC, and BD respectively

Where, X_A, Y_A, X_B, Y_B, X_C, Y_C, X_D, Y_D are reaction in two directions *x* and *y* at joints *A*, *B*, *C*, *D* respectively. The components *A*, *B*, *C*, *D*, *E*, *F*, *G*, *H*, *I*, *J*, *K*, *L*, *N*, *P*, *Q*, *R*, *S*, *T*, *U*, *V* in the expression (1) are provided in details in the Appendix below. In order to determine the relationship between rotational torque of links *AB* and *DC* through chain transmission, let's eliminate 8 variables X_A, X_B, X_C, X_D, Y_A, Y_B, Y_C, Y_D by using the expression $\det(MT) = 0$, where:

$$MT = \begin{bmatrix} A & B & G & H & I & 0 & P & Q & V \\ 1 & 0 & C & 0 & 0 & 0 & 0 & 0 & 0 \\ 0 & 1 & D & 0 & 0 & 0 & 0 & 0 & 0 \\ 1 & 0 & E & -1 & 0 & J & 0 & 0 & 0 \\ 0 & 1 & F & 0 & -1 & K & 0 & 0 & 0 \\ 0 & 0 & 0 & 0 & 0 & 0 & 1 & 0 & R \\ 0 & 0 & 0 & 0 & 0 & 0 & 0 & 1 & S \\ 0 & 0 & 0 & 1 & 0 & L & -1 & 0 & T \\ 0 & 0 & 0 & 0 & 1 & N & 0 & -1 & U \end{bmatrix} \quad (2)$$

From this, it yields:

$$\varepsilon(t)=\ddot{\theta}(t)=-\frac{\left[\left(3\cdot m(t)+m_{BD}\right)\cdot l_1+2m_1l_2\right]\cdot g\cdot\cos\theta(t)+2M}{m_{BD}l_1^2+2m_1l_2^2+2I_{G_1z}} \tag{3}$$

Where, m_1, m_{BD}, and $m(t)$ are mass of links *AB*, *BD* and workpiece respectively, I_{G1z} –moment of inertia mass of two links *AB* and *DC*, *M* is torque used to rotate those two links through chain transmission. According to output requirement, the links will rotate evenly with speed n=15 rpm ($\omega=\pi/2$ rad/s=const, $\theta(t)=\pi t/2$ rad) to ensure the printing productivity of 850 workpieces per hour. When $\varepsilon(t)=0$, it is possible to receive the moment *M* rule in the form as follows [6, 7]:

$$M(t)=-\frac{g}{2}\left[\left(3\cdot m(t)+m_{BD}\right)l_1+2m_1l_2\right]\cos\left(\frac{\pi}{2}t\right) \tag{4}$$

Dynamic reactions at joints *A*, *B*, *C*, *D* are defined in aggrement with the following expression:

$$\begin{aligned}&X_A=\frac{X_A^{nom}}{X_A^{denom}};X_C=\frac{X_C^{nom}}{X_C^{denom}};X_B=\frac{X_B^{nom}}{X_B^{denom}};X_D=\frac{X_D^{nom}}{X_D^{denom}};\\&Y_A=\frac{Y_A^{nom}}{Y_A^{denom}};Y_C=\frac{Y_C^{nom}}{Y_C^{denom}};Y_B=\frac{Y_B^{nom}}{Y_B^{denom}};Y_D=\frac{Y_D^{nom}}{Y_D^{denom}};\end{aligned} \tag{5}$$

The details of numerators and denominators in the expression (5) can be found in the Appendix. The $m(t)$ expresses the mass of workpiece in the frame *BD* at the time of rotating by the arc from period t^* đến t^{**} (bold line), as shown in Figure 3:

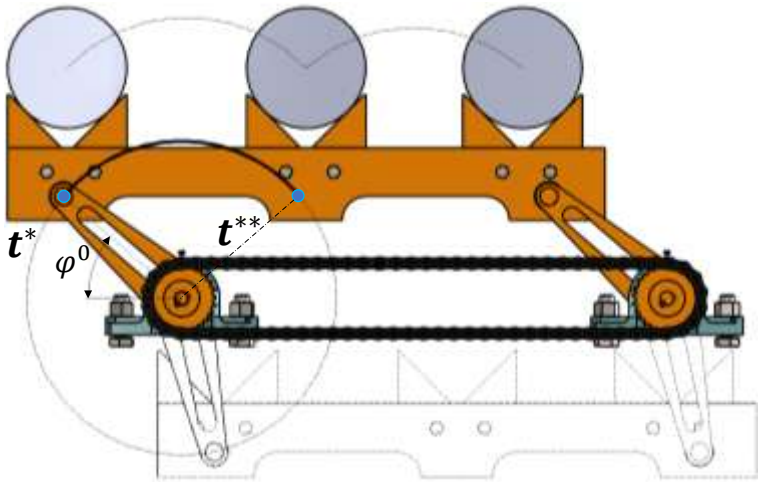

Figure 3. Printer at the position with workpieces

$$m(t)=\begin{cases}m_0 & \text{if } t^*\le t\le t^{**}\\0 & \text{if } t^{**}\le t\le t^*\end{cases} \tag{6}$$

where:

$$t=\begin{bmatrix}t^*=\dfrac{2\varphi_0}{\pi}+2(2k+1)\\t^{**}=4(k+1)-\dfrac{2\varphi_0}{\pi}\end{bmatrix}\quad k=0,\ 1,\ 2,\ \ldots \tag{7}$$

Depending upon the geometry of workpiece, the φ_0 might be varied. According to input data from the design, there are:

$$l_{AB} = l_{CD} = 0.13\,(\mathrm{m}), l_{AG_1} = l_{CG_2} = l_2 = 0.04152\,(\mathrm{m}), l_{BD} = 0.406\,(\mathrm{m}), u_{BG} = 0.20018\,(\mathrm{m}), v_{BG} = 0.02808\,(\mathrm{m}),$$
$$m_{AB} = m_{CD} = m_1 = 0.11888\,(\mathrm{kg}), m_{BD} = 0.8\,(\mathrm{kg}), I_{G_1z} = I_{G_2z} = 259390.5\text{E-}6\left(\mathrm{kg}\cdot\mathrm{m}^2\right), m_0 = 0.2\,(\mathrm{kg})$$

The graphs of reactions at joints *A* in x-direction are illustrated in Figure 4. For the cases of joints *B, C, D*, the graphs have similar charts, but the values and profile are distinctive. The graphs of reactions at joints A in y-direction are presented in Figure 5. For the cases of joints B, C, D, the graphs have similar charts, but the values and profile are varied. Also, the relationship of moment *M* versus time *t* is described in Figure 6. It is important to note that the abrupt variation of curves implies the moment of workpiece presence in the lifting frame.

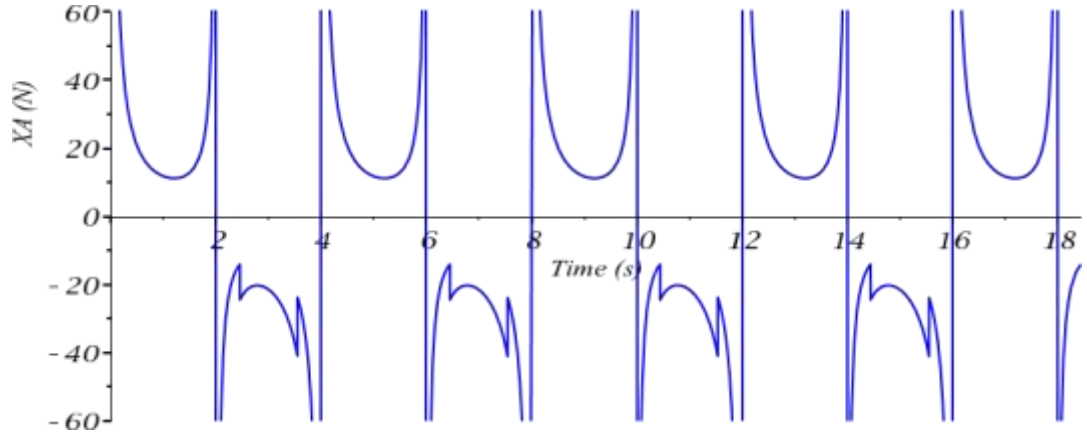

Figure 4. Graphs of reactions at joint A in x-direction

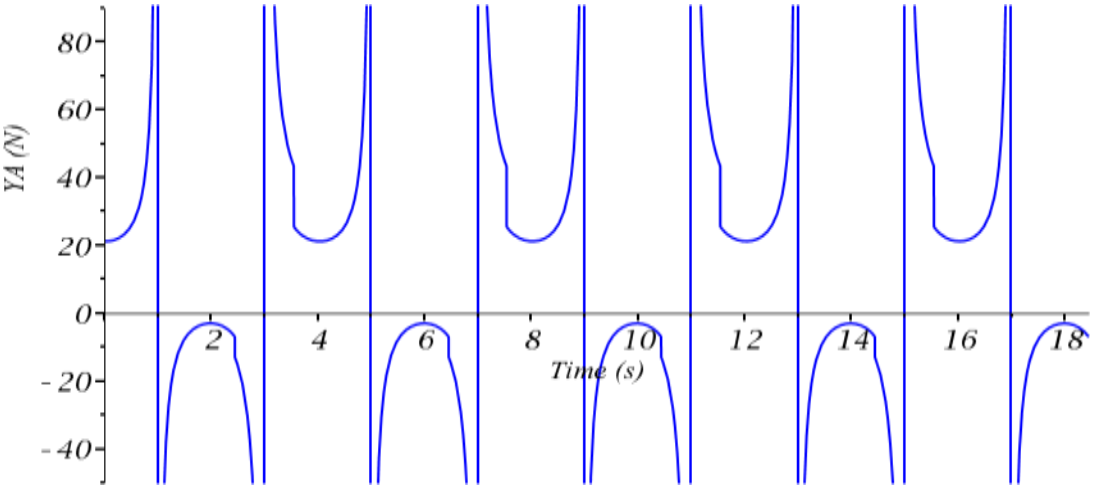

Figure 5. Graphs of reactions at joint A in y-direction

DESIGN OF THE SILKSCREEN PRINTER

Mechanical design

The printer works on the basis of combined six following mechanisms: uniform rotation of a four-bar parallelogram linkage mechanism; sensor activation of the printing system once there is workpiece in; movement of the cylinder lifting the silk frame; linear movement of the cylinder carrying the silk frame; movement of the cylinder lifting squeegee and and ink-coated squeegee; and movement of the cylinder positioning workpiece [8, 9].

It needs to emphasize that the application of the four-bar parallelogram linkage mechanism allows for automation of workpiece feeding and it occurs in a closed-loop procedure that it does not need to have a complicated and costly production line, which in turn economize the working space [10, 11]. Basically, this printer is a combination of mechanical system and control system by cylinder and compression air that would save production and operating costs. Figure 7 shows mechanical system of the printer consisting of the following components:

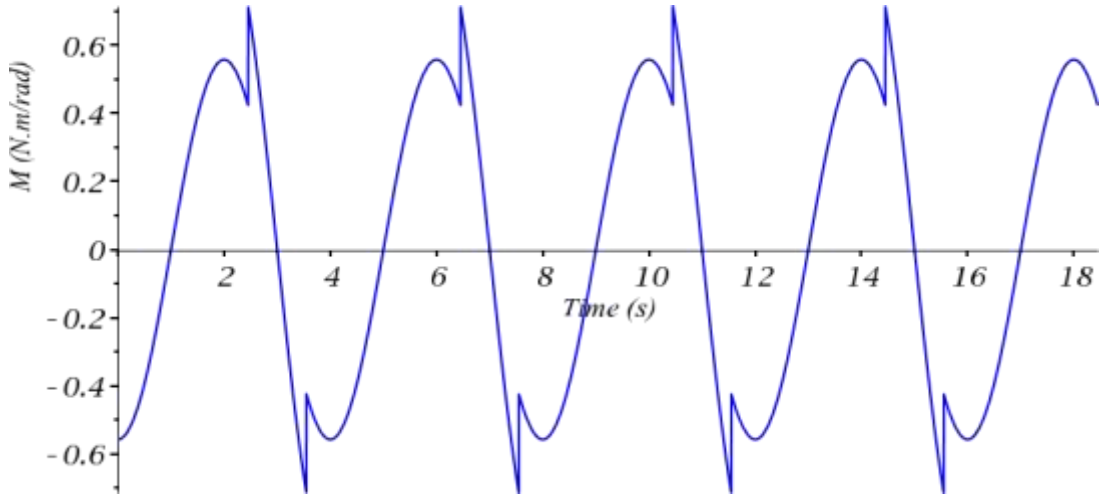

Figure 6. Graphs of moment M

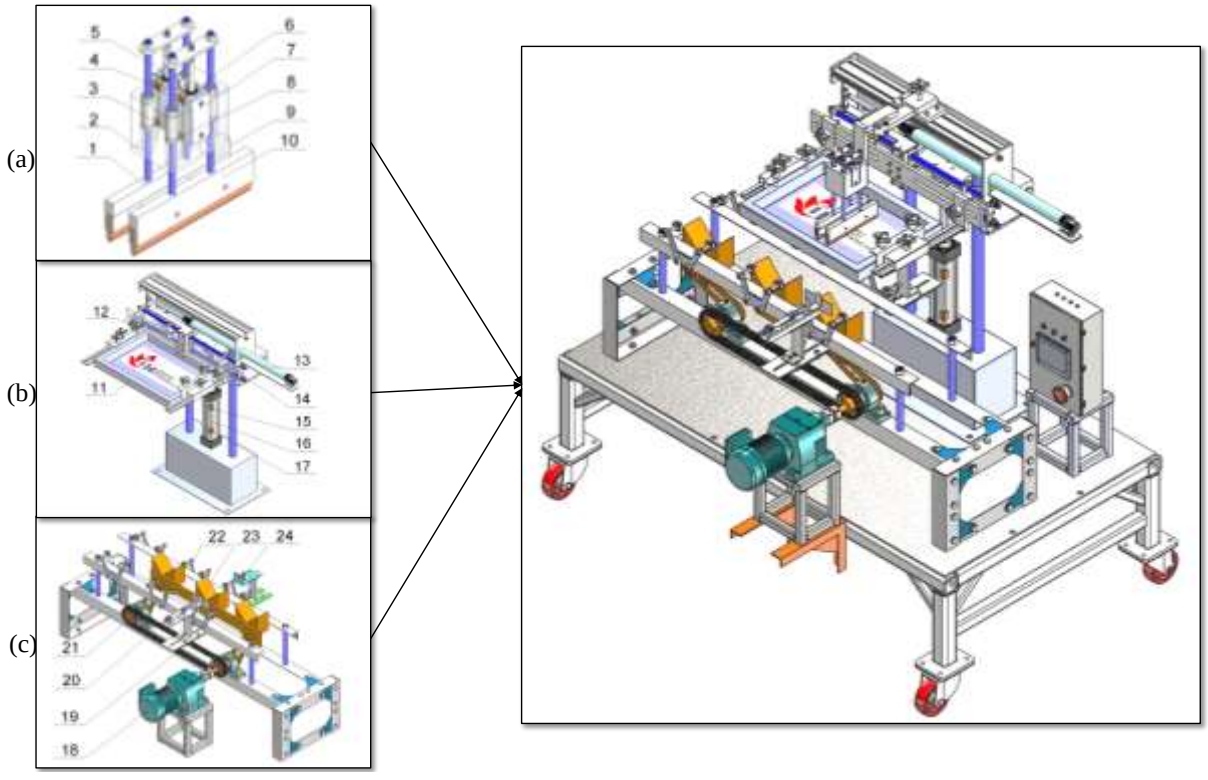

Figure 7. The silkscreen printer

(a)- Print cluster

1- Squeegee
2- Squeegee holder
6- Sensor 3
7- Cylinder lifting the squeegee 2

3- Sensor 1
4- Sensor 2
5- Cylinder lifting the squeegee 1
8- Sensor 4
9- Guide slider
10- Squeegee

(b)- Cluster of print frame lifting structure

11- Silk frame
12- Sensor 5
13- Cylinder guiding silk frame
14- Sensor 6
15- Sensor 7
16- Cylinder lifting the print frame
17- Sensor 8

(c)- Cluster of feeding mechanism

18- Motor
19- Cam chain transmission
20- Cylinder positioning workpiece
21- UPC basement
22- Workpiece attachment
23- Lifting clusters
24- Optical sensor

Control system design

The control circuit diagram of the silkscreen printer is shown in Figure 8. When the printer is connected to the electrical and pneumatic system, the button "start" on the cabinet is pressed, the cotroller will check initial requirements before activating motor operation, namely cylinders (3), (5), (9), (12), (16) are set to the required position.

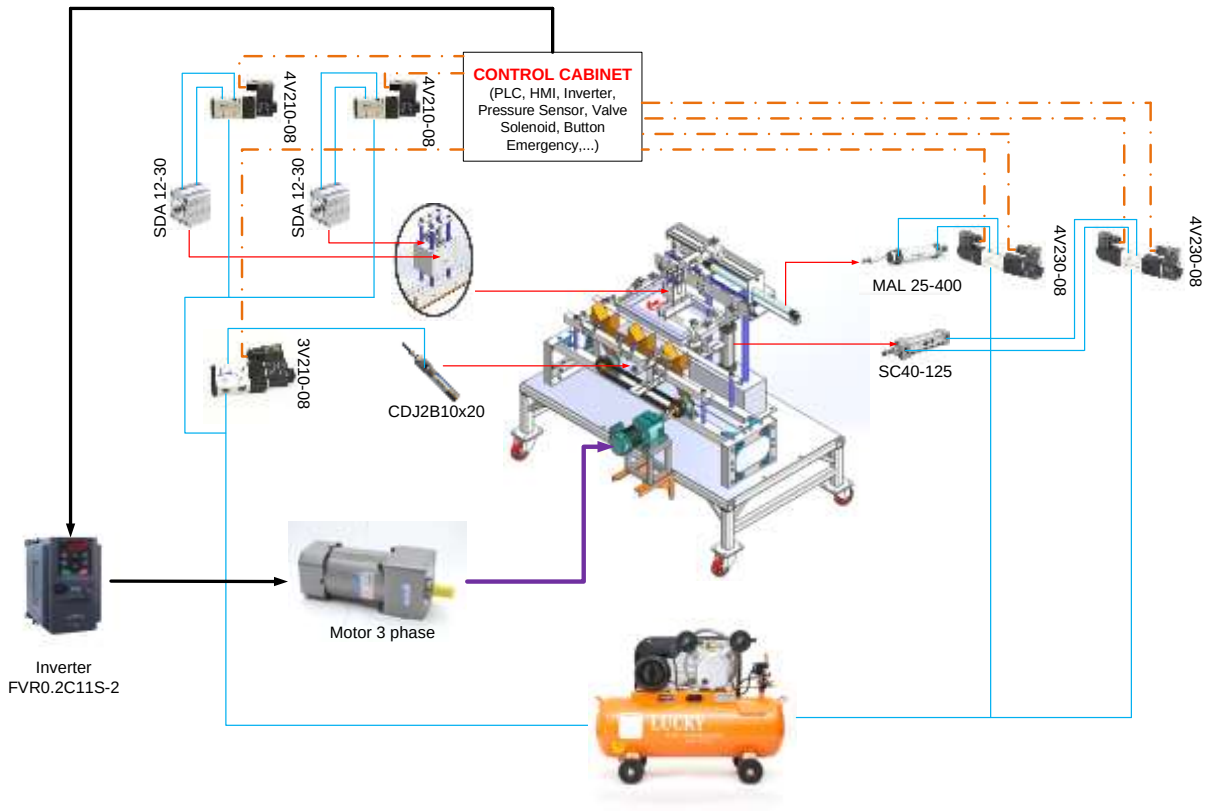

Figure 8. Control circuit diagram of the silkscreen printer

Once the requirement is checked, sensor (11) will activate the motor (14) operation, via chain transmission (15) transmitting rotational movement to the lifting mechanism assembly (19) (by using frequency converter to adjust motor revs). Firstly, position 1 is fed with a workpiece, and then the lifting mechanism (19) approaches to position 1

and lift the workpiece and move to the position 2, here sensor (20) will activate the printing system to operate as shown in Figure 9.

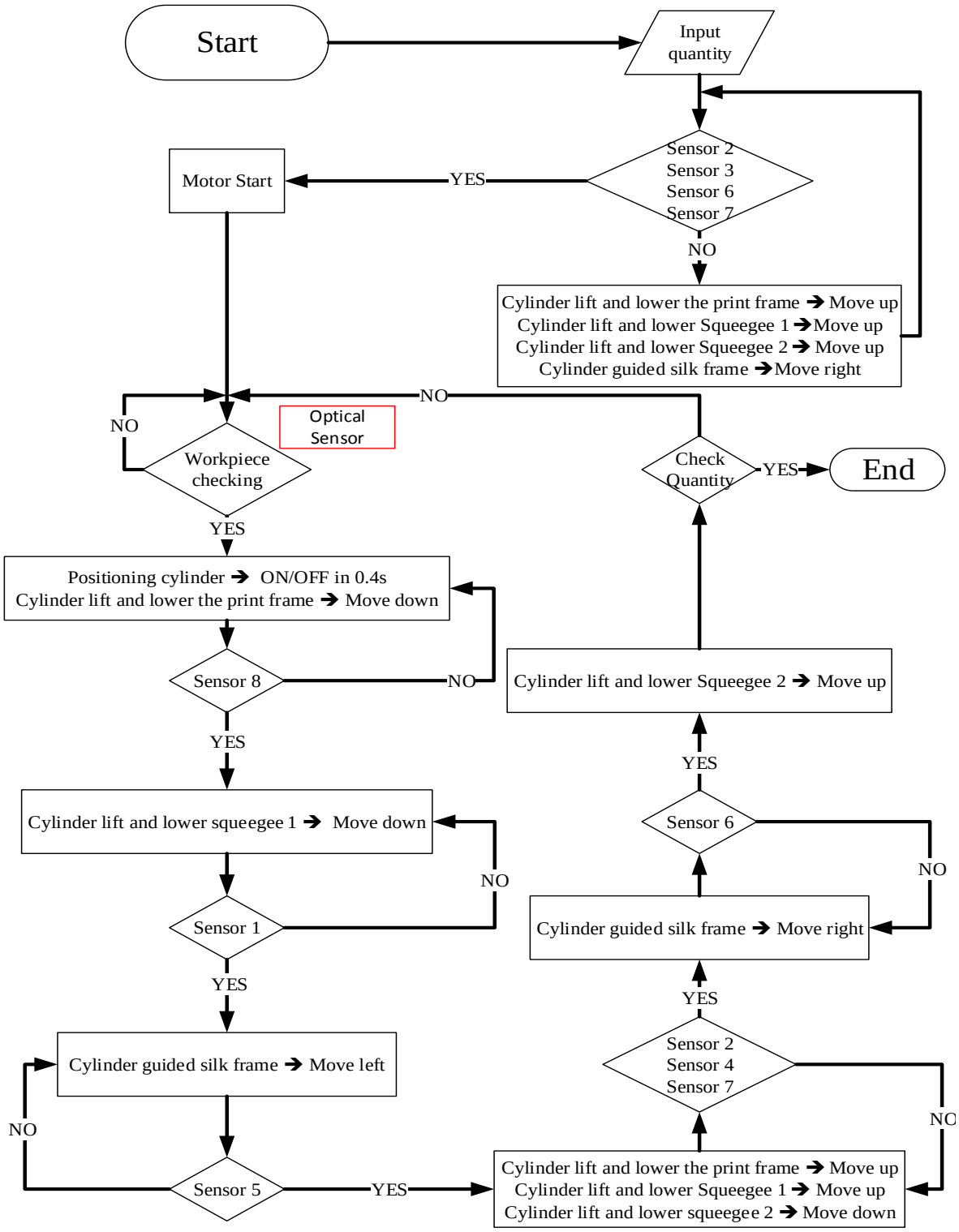

Figure 9. Algorithm diagram for controlling the silkscreen printer

Pace 1: Cylinder (16) place the workpiece exactly at the printing location, at the same time cylinder (12) descends (touch down sensor 13) slowly up to the moment when the silk frame (7) is in contact with the workpiece surface and it stops at this position.

Pace 2: Sensor (13) of cylinder (12) activates cylinder (3) to lower the squeegee (1) being in contact with the silk frame (7) and stops by touching sensor, at this time the squeegee (10) is in the initial state without touching the silk frame.

Pace 3: Once the cylinder (3) touches the sensor and stops, the cylinder (9) will move the silk frame (7) from right to left (touches the sensor (8) then stops) to perform printing.

Pace 4: Sensor (8) activates cylinder (3) to lift the squeegee (1) up to the position without touching the silk plate, the the cylinder (5) bring the squeegee (10) down up to contact with the silk frame, and simultaneously the cylinder (12) lifts the print cluster to touch the sensor (11) then stops.

Pace 5: The sensor (11) activates the cylinder (9) to translate the silk frame (7) going backwards, at this time the ink coating process will be performed (when touching the sensor (10) then stops).

Pace 6: Sensor (10) activates the cylinder (5) to lift the squeegee (10) (a complete printing cycle finishes), then the lifting mechanism (19) moves the printed workpiece in position 2 to position 3, where the worker take out the final product, at the same time the lifting mechanism (19) continues to work to bring the new workpiece at position 1 to position 2 and the process repeats again and forms a closed cycle.

MANUFACTURE, TEST AND PERFORMANCE EVALUATION OF THE PROTOTYPE

Figure 10 shows principal parts of the printer. Once these parts were manufactured, they were assembled to create a complete printer, as demonstated in Figure 11. After that, printing experiment was carried out, as shown in Figure 12a. The printer has performed as desgined in term of productivity and product quality. Figure 12b shows one of the printed product after the printing experiment. Print quality actually met the requirements for uniform ink distribution without blurring. In case, it need to print cylindrical workpiece with different diameters and lengths, the user only has to adjust the silk frame height (the stroke of the cylinder lifting the silk frame).

(*a*)

(*b*)

(*c*)

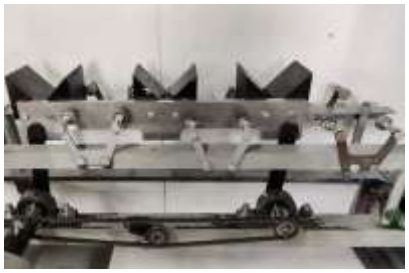

(*d*) (*e*) (*f*)

Figure 10. Principal parts of the silkscreen printer: (*a*) – Components for moving silk frame; (*b*) – Squeegees; (*c*) – Silk frame; (*d*) – Lifting mechanism; (*e*) – Transporting mechanism; (*f*) – Control cabinet

Figure 11. Prototype of the silkscreen printer developed in this study

(*a*) (*b*)

Figure 1. (*a*) – Printing experiment; (*b*) – Final product after printing

CONCLUSION

This paper introduced the design and development of an innovative silkscreen printer with automatic mechanism of feeding and transporting workpieces. Dynamic model of mechanism of feeding and transporting workpieces was developed. The model has made a firm basis for calculation and selection of motor. Based on the design, the printer prototype was manufactured, assembled and tested for verification. Printing experiment indicated that the printer has performed successfully with the productivity as designed. This newly printer showed many advantages in terms of cost, compact size, high technology, mass printing with high productivity and ability to respond to many other shapes and sizes of workpiece. The printer configuration is suitable for small and medium-sized businesses companies, promising to have a lot of competitive potential in the silkscreen printer market.

ACKNOWLEDGEMENT

The contribution to this paper and financial support from Industrial University of Ho Chi Minh City, Vietnam under the research project no. 20/1.1CK04 is highly acknowledged.

APPENDIX

Formula of components mentioned in the Section 2.2:

$$A = -m_1 l_2 \left(\ddot{\theta} \sin\left(\theta(t)\right) + \left(\dot{\theta}(t)\right)^2 \cos\left(\theta(t)\right) \right); B = m_1 g + m_1 l_2 \left(\ddot{\theta} \cos\left(\theta(t)\right) - \left(\dot{\theta}(t)\right)^2 \sin\left(\theta(t)\right) \right);$$

$$C = -y_A + y_{G_1}; D = x_A - x_{G_1}; E = -y_B + y_{G_1}; F = x_B - x_{G_1}; G = M + I_{G_1 z} \ddot{\theta}(t);$$

$$H = -m_{BD} l_1 \left(\ddot{\theta}(t) \sin\left(\theta(t)\right) + \dot{\theta}^2 \cos\left(\theta(t)\right) \right);$$

$$I = m_{BD} g + m_{BD} l_1 \left(\ddot{\theta}(t) \cos\left(\theta(t)\right) - \dot{\theta}^2 \sin\left(\theta(t)\right) \right) + 3m(t)g; J = y_B - y_G;$$

$$K = -x_B + x_G; L = -y_D + y_G; N = x_A - x_G; P = -m_1 l_2 \left(\ddot{\theta}(t) \sin\left(\theta(t)\right) + \dot{\theta}^2 \cos\left(\theta(t)\right) \right);$$

$$Q = m_1 g + m_1 l_2 \left(\ddot{\theta}(t) \cos\left(\theta(t)\right) - \dot{\theta}^2 \sin\left(\theta(t)\right) \right); R = -y_C + y_{G_2}; S = x_C - x_{G2};$$

$$T = y_D - y_{G2}; U = -x_D + x_{G_2}; V = M + I_{G_1 z} \theta(t)$$

Where, coordinator of joints is defined as follows:

$$x_A = 0; y_A = 0; x_B = l_1 \cdot \cos\left(\theta(t)\right); y_B = l_1 \cdot \sin\left(\theta(t)\right); x_C = l_{BD}; y_C = 0;$$

$$x_D = l_1 \cdot \cos\left(\theta(t)\right) + l_{BD}; y_D = l_1 \cdot \sin\left(\theta(t)\right); x_G = l_1 \cdot \cos\left(\theta(t)\right) + u_{BG}; y_G = l_1 \cdot \sin\left(\theta(t)\right) + v_{BG};$$

$$x_{G1} = l_2 \cdot \cos\left(\theta(t)\right); y_{G1} = l_2 \cdot \sin\left(\theta(t)\right); x_{G_2} = l_2 \cdot \cos\left(\theta(t)\right) + l_{BD}; y_{G_2} = l_2 \cdot \sin\left(\theta(t)\right);$$

$$X_A^{nom} = AJS + AJU - AKR - AKT + ALS + ALU - ANR - ANT - HKR - HKT + HLS + HLU - HNR - HNT - IKS - IKU - KPR - KQS - NPR - NQS + KV + NV;$$

$$X_A^{denom} = JS + JU - KR - KT + LS + LU - NR - NT;$$

$$Y_A^{nom} = BJS + BJU - BKR - BKT + BLS + BLU - BNR - BNT + HJR + HJT + IJS + IJU + ILS + ILU - INR - INT + JPR + JQS + LPR + LQS - JV - LV;$$

$$Y_A^{denom} = JS + JU - KR - KT + LS + LU - NR - NT;$$

$$X_B^{nom} = HKR + HKT - HLS - HLU + HNR + HNT + IKS + IKU + KPR + KQS + NPR + NQS - KV - NV;$$

$$X_B^{denom} = JS + JU - KR - KT + LS + LU - NR - NT;$$

$$Y_B^{nom} = -HJR - HJT - IJS - IJU - ILS - ILU + INR + INT - JPR - JQS - LPR - LQS + JV + LV;$$

$$Y_B^{denom} = JS + JU - KR - KT + LS + LU - NR - NT;$$

$$X_C^{nom} = HJS + HJU + IKS + IKU + JPS + JPU - KPT + KQS + LPS + LPU - NPT + NQS - KV - NV;$$

$$X_C^{denom} = JS + JU - KR - KT + LS + LU - NR - NT;$$

$$Y_C^{nom} = -HJR - HJT - IKR - IKT - JPR + JQU - KQR - KQT - LPR + LQU - NQR - NQT + JV + LV$$

$$Y_C^{denom} = JS + JU - KR - KT + LS + LU - NR - NT;$$

$$X_D^{nom} = HJS + HJU + IKS + IKU + KPR + KQS + NPR + NQS - KV - NV;$$

$$X_D^{denom} = JS + JU - KR - KT + LS + LU - NR - NT;$$

$$Y_D^{nom} = -HJR + HJT - IKR - IKT - JPR - JQS - LPR - LQS + JV + LV;$$

$$Y_D^{denom} = JS + JU - KR - KT + LS + LU - NR - NT;$$

REFERENCES

[1] C. MiIo, V.F. Filzi, E. Reggio, R. Vittorio. A Silk Screen Printing Machine For Cylindrical Objects, Italy Patent, 2007.

[2] N. Mitsunori, Screen Printing Machine And Solar Battery Cell, Mitsubishi Electric Corporation, Patent, 2011.

[3] S.A. Kacharen, N.N. Narwade, V.U. Mandle, H.V. Shiraskar, V.P. Sawant. Pneumatic Multicolour Screen Printing Machine, Patent, 2016.

[4] G.R. Selase, V. Divine, D. Elorm, A. Joseph, A.F Emefa, A. Joana. Portable T-Shirt Printing Machine, Patent, 2017.

[5] H.M. Dang, V.P. Bui, V.B. Phung, S.S. Gavriushin, V.D. Nguyen, PAMMS - Procedure for Automation of Mathematical Modeling and Solution of Mechanical system: Application for the Design of an Innovative Fruit and Vegetable Washer. Journal of Mechanical Engineering Research and Developments, vol. 43, no. 3, Pp. 429-442, 2020.

[6] N. Pandrea and D. Popa. Classical and Modern Approaches in the Theory of Mechanisms, John Wiley and Sons, 2017.

[7] M. J. Rider. Design and analysis of mechanisms: a planar approach, John Wiley & Sons, Ltd, 2015.

[8] S. M. Varedi, H. M. Daniali, M. Dardel. Dynamic synthesis of a planar slider–crank mechanism with clearances. Nonlinear Dynamics, No. 79, pp. 1587–1600, 2015.

[9] A. A. Jomartov, S. U. Joldasbekov, and Yu. M. Drakunov, Dynamic synthesis of machine with slider-crank Mechanism. Mechanical Sciences, No. 6, pp. 35–40, 2015.

[10] G. Dieter and L. Schmidt. Engineering Design, 5th Edition, McGraw-Hill Higher Education, 2012.

[11] M.-S. Huang, K.-Y. Chen, R.-F. Fung, Comparison between mathematical modeling and experimental identification of a spatial slider–crank mechanism, Applied Mathematical Modelling, No. 34, pp. 2059–2073, 2010.